NHE6 AND NHE9 ARE SODIUM HYDROGEN EXCHANGERS FOUND ON SEPARATE MOBILE ENDOSOME POPULATIONS IN NEURONAL DENDRITES

Mark Guterman

A Thesis
in
The Department
of
Biology

Presented in Partial Fulfillment of the Requirements
for the degree of Master of Science (Biology) at
Concordia University
Montreal, Quebec, Canada

September 2013

CONCORDIA UNIVERSITY

School of Graduate Studies

This is to certify that the thesis prepared

By: Mark Guterman

Entitled: NHE6 and NHE9 are sodium hydrogen exchangers found on separate mobile endosome populations in neuronal dendrites

and submitted in partial fulfillment of the requirements for the degree of

Master of Science (Biology)

complies with the regulations of the University and meets the accepted standards with respect to originality and quality.

Signed by the final Examining Committee:

_____ Chair
Dr. David Walsh

_____ Examiner
Dr. Alisa Piekny

_____ Examiner
Dr. Andrew Chapman

_____ Examiner
Dr. Madoka Gray-Mitsumune

_____ Supervisor
Dr. Christopher Brett

Approved by _____
Chair of Department or Graduate Program Director

_____ 2013 _____
Dean of Faculty

ABSTRACT

NHE6 And NHE9 Are Sodium Hydrogen Exchangers Found On Separate Mobile Endosome Populations In Neuronal Dendrites

Mark Guterman, M.Sc.

This dissertation reports the endosomal locations of NHE6 and NHE9, sodium hydrogen exchangers that contribute to pathogenesis of Autism Spectrum Disorders (ASDs) within dendrites of cultured hippocampal neurons. ASDs are debilitating, neurological disorders characterized by deficient social interaction; obsessive, repetitive behaviors; and often accompanied by mental retardation, epilepsy, and attention deficit hyperactivity disorder (ADHD). For normal brain function to occur neurons form circuits at synapses and their size and strength change based on use, known as synaptic plasticity. Disruption of synaptic plasticity is thought to underlie ASDs. Because endocytosis is required for synaptic plasticity and the yeast ortholog of human Nhe6 and Nhe9 is known to contribute to this process, I hypothesized that Nhe6 and Nhe9 are found on endosomes in hippocampal neurons where they contribute to endocytosis and synaptic plasticity. Using fluorescence microscopy, I initially demonstrate that Nhe6 and Nhe9 are localized to different pools of endosomes with cultured HeLa cells using Rab-GTPases as markers of the endocytic pathway. Nhe6 and Nhe9 showed similar distribution within the dendrites of hippocampal neurons cultured from mice or rats whereby Nhe6 was present in Rab5 and Rab11-positive endosomes and Nhe9 was found in Rab11, Rab7, and Rab9-positive endosomes later in the pathway. Live

neuron imaging revealed that both Nhe6 and Nhe9 endosomes are mobile and that Nhe9-positive endosomes appear to undergo transient fusion and fission events from Rab7, Rab9, or Rab11-positive endosomes. Together, these data imply roles for Nhe6 and Nhe9 in endosome mobility and fusion underlying endocytosis required for synaptic plasticity.

ACKNOWLEDGEMENTS

First and foremost, I would like to thank my supervisor Dr. Christopher Brett for the opportunity, and his support and encouragement throughout my tenure. Thank you for helping me develop the tools necessary to become an independent researcher, presenter, and writer. Your passion and drive for science is an inspiration and I am glad to have been a part of it. I would also like to thank my committee members Dr. Alisa Piekny and Dr. Andrew Chapman for their helpful discussion and support.

Financial support for this project was provided by Canada Research Chairs, which was very much appreciated.

I want to extend my thanks to the manager of our lab and the head of the Center for Microscopy at Concordia, Gabriel Lapointe. Thank you for all of your training and patience to help me become the scientist I am today.

Thanks to my fellow graduate students Mahmoud Karim, Joël Richard, and Dipti Patel for always having someone to bounce ideas off of and someone to complain to when experiments wouldn't work.

I would like to thank my family: Abraham and Erica Guterman, and Karen, Craig, and Sam Kirsner for their endless love and support. Without all of you, none of this would have been possible. I'd also like to thank my girlfriend and friends, whose love and motivation kept me going when times were tough.

Finally, I would like to thank coffee and beer: coffee to get me started and going through the day and beer for winding down after especially long weeks.

Table of Contents

List of Figures

1. Introduction

1.1 $Na^+(K^+)/H^+$ Exchangers and ASDs

Autism Spectrum Disorders (ASDs) encompass a range of heritable, psychiatric diseases that are characterized by impaired communication and social interaction; repetitive behaviors; and narrow, obsessive interests. Patients with severe forms of the disease also present mental retardation, attention deficit hyperactivity disorder (ADHD), and epilepsy (Morrow et al., 2008; Toro et al., 2010). Currently, mutations in over thirty genes are linked to ASDs that target genes with predicted functions in membrane adhesion, autophagy, and endocytosis – processes that change the number, size, and strength of synapses, otherwise known as synaptic plasticity. Synaptic plasticity in humans is crucial at young ages, when brain growth slows and synapses are pruned to refine the neural networks responsible for cognition, learning, and memory.

A subset of mutations linked to ASDs target the endosomal $Na^+(K^+)/H^+$ exchangers (NHEs) NHE6 and NHE9 (Morrow et al., 2008; Zhang-James et al., 2011). Mutations in NHE6 have been shown to underlie the rare, X-linked disorder known as Christianson Syndrome, a severe ASD in which patients present with severe mental retardation, microcephaly, ataxia, and cerebellar atrophy (Gilfillan et al., 2008) (Mignot et al., 2012). An NHE6 knockout mouse has shown to present Christianson Syndrome-like phenotypes such as ataxia, due to cerebellar atrophy, mainly due to Purkinje cell loss, confirming that this mutation contributes to pathogenesis (Strømme et al., 2011). Mutations in NHE9 are linked to autism and

ADHD (Morrow et al., 2008; Zhang-James et al., 2011). Both NHE6 and NHE9 transcripts are found in subpopulations of neurons in regions of the adult mouse brain associated with ASDs, such as the cortex, hippocampus, and cerebellum – areas important for cognition, behavior, learning, and memory (Lein et al., 2007). Furthermore NHE6 transcripts are more wide-spread than NHE9, in support of the observation that disease phenotypes associated with NHE6 mutations are more severe.

Recently, NHE6 was shown to be present in hippocampal CA1 pyramidal neurons within distinct intracellular puncta, which can be stained with transferrin (Deane et al., 2013), a marker of the endocytic pathway. However, it has not been shown whether NHE9 protein is expressed in neurons and the function of these two proteins has yet to be explored. Based on this preliminary finding and results from studies in cultured cell lines, it has been proposed that NHE6, and possibly NHE9, may contribute to endocytosis (Xinhan et al., 2011). This cellular process is critical for synaptic plasticity by regulating neurotransmitter receptor surface levels at dendritic spines – small protrusions in dendrites acting as post-synaptic compartments (Park et al., 2006). As defects in plasticity are thought to underlie ASDs (Ebert and Greenberg, 2013), I hypothesize that mutations in NHE6 or NHE9 may disrupt endocytosis and receptor recycling required for synaptic plasticity, leading to symptoms associated with ASDs.

1.2 Synaptic plasticity, endocytosis, and NHEs

Neurons are polarized cells with unique features: an axon which ends with the terminal pre-synapse and contains the molecular apparatus to propagate an

action potential and neurotransmitter release; and dendrites, the post-synaptic component that receives input from neighboring axons using neurotransmitter receptors (Kennedy and Ehlers, 2006). Neurons form circuits in the brain through synapses, sites of neuronal communication.

Synapses are dynamic and change size and strength based on use (Kennedy and Ehlers, 2006). Post-synaptic remodeling at dendritic spines requires reorganization of the actin cytoskeleton and scaffold proteins to change shape and size and movement of neurotransmitter receptors on and off the post-synaptic membrane to change synaptic strength. This plasticity is a cumulative phenomenon and also depends on the history of the synapse, thus is believed to be the foundation of learning, memory, and cognition (Bliss and Collingridge, 1993; Malenka and Nicoll, 1999; Malenka and Bear, 2004).

Endosomes in dendritic spines are important for maintaining a mobilizable pool of synaptic neurotransmitter receptors and membrane for synaptic plasticity (Newpher and Ehlers, 2008). When dendritic spines undergo long-term potentiation (LTP; long-lasting increase in synaptic size and strength), membrane trafficking from recycling endosomes to the post synaptic membrane is required for spine growth and maintenance (Park et al., 2006). Conversely, internalization of the postsynaptic membrane by endocytosis underlies synaptic pruning (Kennedy and Ehlers, 2006). Although the precise sub-cellular locations of Nhe6 and Nhe9 are unknown in neurons, they have been localized to endosomes in cultured cell lines where they regulate endosomal pH and receptor recycling (Brett et al., 2002; Nakamura et al., 2005 Hill et al., 2006).

1.3 NHE6 and NHE9 are found on endosomes in mammalian cells

NHEs (also known as SoLute Carrier 9A, SLC9A) are found in all organisms and are integral membrane transport proteins. They have a role in numerous functions involving cellular pH, salt, and volume homeostasis in which they contribute to diverse physiology and are part of the cation protein antiporter (CPA) superfamily (Brett et al., 2005a). These proteins are secondary active ion transporters which perform electroneutral activity by transporting H^+ in exchange for monovalent cations across membranes, down their concentration gradients (Brett et al., 2005a). To date, nine isoforms have been found in mammals in which they all contain an evolutionarily conserved 12 transmembrane domain region at the amino terminus and a variable tail at the carboxyl terminus in which regulatory proteins can interact and bind (Brett et al., 2005a; Ohgaki et al., 2008). Mammalian NHEs have been classified into two broad categories based on location: plasma membrane and intracellular. NHE1-5 are more closely related to each other and are commonly localized to the plasma membrane whereas NHE6-9 share more similarity to each other where they function at intracellular compartments.

Intracellular NHEs in mammals are further subdivided into two clades: NHE8-like NHEs (NHE8, and the endosomal/*trans*-Golgi network (TGN) NHEs, which include the endosomal NHE6, 7, and 9 (Brett et al., 2002; Brett et al., 2005a; Hill et al., 2006). The intracellular NHEs 6,7, and 9 are approximately 60% similar in amino acid sequence (Nakamura et al., 2005) and their ancestry can be traced to NHX1 in *Saccharomyces cerevisiae* (Brett et al., 2005a). NHE6, 7 and 9 have mostly been studied in mammalian cell culture lines, whereby NHE6 and NHE9 have been

shown to localize to early and recycling endosomes and dictate endosomal pH (Numata and Orlowski, 2001; Brett et al., 2002; Nakamura et al., 2005; Ohgaki et al., 2008, 2010), and NHE7 has been predominantly localized to the TGN (Numata and Orlowski, 2001). Unfortunately, this is the extent of our knowledge with regards to the cellular functions of NHE6 and 9. Thus, to gain insight, we turn to the yeast ortholog of these exchangers, Nhx1 whose function in the endocytic pathway has been better resolved.

1.4 Nhx1, Rab-GTPases, and endocytosis in yeast

Like Nhe6, 7 and 9, Nhx1 localizes to endosomes and the TGN in yeast and regulates trafficking of protein cargoes in the endocytic pathway (Kojima et al., 2012). Loss of function mutations in NHX1 result in accumulation of internalized surface receptors, such as Ste3, a G-protein coupled receptor (Bowers et al., 2000; Ali et al., 2004; Brett et al., 2005b) in an abnormally endosome compartment, preventing degradation. Like NHE6 and NHE9, Nhx1 activity counters the V-ATPase to alkalinize the lumen of endosomes, and H+-transport by Nhx1 is known to be critical for its roles in endocytic trafficking (Ali et al., 2004; Brett et al., 2005b). Most importantly, Nhx1 binds to Gyp6, a Rab-GTPase Activating Protein (Rab-GAP), that regulates the activity of two Rab-GTPases known to drive membrane trafficking out of the endosome: Ypt6 (the yeast ortholog of human Rab9), which mediates endosome-TGN fusion required for receptor recycling, and Ypt7 (the yeast ortholog of human Rab7) which mediates endosome - lysosomal vacuole fusion required for receptor degradation (Stenmark, 2009; Brett et al., 2008; Balderhaar et al., 2010; Epp et al., 2011). Given that Nhx1 regulates Rab-GTPase signaling to control

membrane fusion events underlying endocytosis, I hypothesize that mammalian NHE6 and NHE9 may perform similar functions in neuronal dendrites to regulate synaptic plasticity. To test this hypothesis, I examined the distribution of NHE6 and NHE9 first in cultured HeLa cells, and then in hippocampal neurons cultured from rodents using fluorescence microscopy to: (1) identify the Rab-positive compartments harbor NHE6 or NHE9; (2) determine if NHE6 or NHE9-positive endosomes are present in neuronal dendrites, and (3) document NHE6 or NHE9-positive endosomes undergoing fusion or fission events with Rab-GTPase-positive compartments in the endocytic pathway.

2. Materials and methods

2.1 Cell culture

2.1.1 Neuronal cell culture

2.1.1.1 Coverslip preparation

To promote neural cell adhesion, glass coverslips (12 mm circle, #1.5, Fisher Scientific) were soaked in > 90% fuming nitric acid overnight and washed with water prior to sterilization. The sterile coverslips were then coated with poly-$_D$-lysine (30 μg/mL; Millipore) and laminin (3 μg/mL; Millipore) diluted in borate buffer (50 mM boric acid at pH 8.5) by incubation at 37°C for 4 hours. After 5 washes with sterile water, the coated coverslips were placed in Dulbecco's Modified Eagle's Medium (DMEM; Multicell) supplemented with 10% fetal bovine serum (FBS; Multicell) in preparation for neuronal culture.

2.1.1.2 Neuron culture

Hippocampi were isolated from embryonic, day 18-19 Sprague-Dawley rats, purchased from Charles River Laboratories (Wilmington, MA, USA), in Hank's Balanced Salt Solution (HBSS) (Multicell) (supplemented with 1 mM sodium pyruvate, 100 mM HEPES at pH 7.4, and Penicillin-Streptomycin [1,000 units Penicillin, 85.9 mM Streptomycin]) and incubated in 5 mL Trypsin/EDTA solution (0.25%, 0.1% respectively, Multicell) for 15 minutes at 37°C. The hippocampi were subsequently washed three times in 5 mL HBSS for 5 minutes, then brought to a final volume 1 mL. The hippocampi were dissociated via trituration by a series of flame-narrowed Pasteur pipettes and then the cells were counted with a solution of trypan blue (0.4% solution in phosphate buffered saline, Multicell) on a

hematocytometer (Bright-Line, Hausser Scientific, Horsham, PA, USA). The cells were plated at a density of 442 cells/mm^2 on treated coverslips. Once plated, the cells were incubated for 4 hours at 37°C, 8% CO_2, after which the media was changed to Neurobasal (Multicell), 2% B27 (Invitrogen), 1% GlutaMAX (Invitrogen), and 1μL glutamate 25 mM. After 3 days, and for every 2-3 days following, half of the media was replaced with maintenance media (Neurobasal, 2% B27, 1% GlutaMAX).

Neurons for live imaging were isolated from post-natal, day 2 mice, strain C57BL/6 originally purchased from Jackson Laboratories (Bar Harbor, ME, USA) in HBSS. The procedure to isolate hippocampal neurons was the same from rats albeit with a few alterations. During isolation, the hippocampi were incubated in 5 mL HBSS with 165 units of Papain and 15,000 units of DNase for 30 minutes at 37°C. The Papain-DNase mixture was removed and the hippocampi were washed once in HBSS and twice in 5 mL DMEM with FBS for 5 minutes each, with the final volume being brought to 2 mL. The hippocampi were dissociated as previously mentioned, but then centrifuged at 300*g* for 5 minutes and re-suspended in 5 mL DMEM and FBS. The cells were counted as previously mentioned and plated at a density of 1,966 cells/ mm^2 on 18 mm, #1.5 cover slips (Fisher Scientific).

2.1.2 HeLa culture

HeLa cells were maintained in DMEM with 10% Cosmic Calf Serum (Fisher Scientific) and L-glutamine (2 mM) in a 10 cm Petri dish. During passage, cells were washed with phosphate-buffered saline (PBS) (Multicell), and then incubated with 0.05% Trypsin/EDTA for 5 minutes at 37°C to promote detachment of the cells from the plate. The same volume of media was then added, and the whole mixture was

mixed, while ensuring cell detachment from the plate. The mixture was then centrifuged at 300*g* for 5 minutes and re-suspended in 10 mL of fresh media. One mL of re-suspended cells was then plated into 9 mL fresh media in a new, sterile 10 cm Petri dish.

2.1.3 Transfections

2.1.3.1 HeLa transfection

Cultured HeLa cells were grown to confluency between 60-80% on sterile, non-treated coverslips in a 24-well tissue culture plate (Corning Incorporated, Corning, NY, USA). The media was changed 30-60 minutes prior to transfection and then transfected using polyethylenimine (PEI) (linear, MW 25 kD, Polysciences Inc., Warrington, PA, USA). Each coverslip was transfected using 0.3 µg plasmid DNA and 2.5 µg PEI in a total volume of 40 µL of supplement-free media (DMEM) and incubated for 3-6 hours at 37°C, 5% CO_2. After incubation, the cells were rinsed twice with PBS, and incubated in fresh, supplemented media overnight at 37°C, 5% CO_2.

2.1.3.2 Neuron transfection

Cultured neurons that were plated at 442 cells/mm^2 on prepared coverslips in a standard 24-well tissue culture plate were transfected with lipofectamine 2000 (Invitrogen) at day *in vitro* (DIV) 9-10. For each well, 2 µL of lipofectamine 2000 was hydrated into 75 µL unsupplemented Neurobasal medium for at least 5 minutes at room temperature. A separate mix of 1 µg of plasmid DNA was mixed with 75 µL unsupplemeneted Neurobasal medium. The two solutions were mixed together and

incubated for 20 minutes at room temperature. The media from the well was removed, but saved, and the transfection mix was plated and incubated for 10 minutes at 37°C, 8% CO_2. During the incubation period, the saved media was brought to a final volume of 500 µL per well with supplemented Neurobasal. After 10 minutes, the transfection mix was removed from the wells and replaced with 500 µL Neurobasal and incubated overnight at 37°C, 8% CO_2.

2.2 Staining

2.2.1 Fixation

HeLa cells were fixed the day after transfection and neurons were fixed at DIV 14-15. The culture plate was placed on ice and the cells were washed twice with ice cold PBS (HeLa) or HBSS (neurons). The cells were then fixed in a freshly made solution of PBS containing 4% paraformaldehyde (PFA) and 4% sucrose at a pH of 7.4 by keeping the plate on ice for 30 minutes and then placed at room temperature for 15-30 minutes. The fixative was removed and the cells were washed twice with room temperature PBS or HBSS for at least 10 minutes each.

2.2.2 DAPI stain

Post fixation, the nuclei of HeLa cells were counterstained with 50 ng/mL 4',6-diamino-2-phenylindole (DAPI) for 5 minutes at room temperature, then washed again with PBS. The coverslips were then mounted on 1 mm thick microscope slides (Unifrost) with Prolong Gold Anti-fade Reagent (Invitrogen) and cured in the dark for at least 3 hours. The coverslips were then sealed with dark nail polish, allowed to dry, then stored at 4°C prior to imaging.

2.3 Antibodies

Affinity-purified anti-Nhe6 rabbit polyclonal antibodies were raised against the C terminus (GDHELVIRGTRLVLPMDDSE) of human NHE6 isoform b (amino acid residues 636-655). Affinity-purified anti-Nhe9 rabbit polyclonal antibodies were generated from the C terminus (SPSPSSPTTKLALDQKSSGC) of mouse Nhe9 with an added C-terminal cysteine (amino acid residues 594-612). Both antibodies were obtained as a generous gift from Dr. Peter Gillespie (OHSU, Oregon, USA) with the antibody to Nhe9 being generated by Genemed Synthesis (San Francisco, CA, USA).

The following additional primary antibody was used: mouse monoclonal anti-PSD95 (Sigma). The following secondary antibodies were used: Alexa Fluor 568 or Alexa Fluor 647-conjugated donkey anti-mouse and Alexa Fluor 647-conjugated donkey anti-rabbit (Invitrogen).

2.3.1 Immunofluorescence

Cultured HeLa cells and neurons were fixed in 4% PFA, and then permeabilized with 0.1% TritonX-100 and 1% glycine in PBS for 15 minutes two times at room temperature. The cells were then blocked with 1% bovine serum albumin (BSA) in PBS-Tween-20 (PBST) (0.1% Tween-20 in PBS) for at least 30 minutes at room temperature followed by incubation with primary antibodies in PBST with 1% BSA (anti-Nhe6 1:100, anti-Nhe9 1:200) overnight at 4°C. The cells were washed twice with PBST with 1% BSA for 15 minutes at room temperature and then incubated with fluorescently labeled secondary antibodies in PBST containing 1% BSA (all 1:400) for 2 hours at room temperature. After 4 washes with

PBST containing 1% BSA of 15 minutes each, the coverslips were mounted on microscope slides with Prolong Gold in the same manner as previously stated.

2.4 Image analysis

HeLa cell images were acquired on a Nikon Ti-E inverted microscope using a photometrics KINO camera with a 60X Plan Apo lambda oil immersion objective (with a numerical aperture of 1.4) using a BCECF filter to detect GFP signal at an emission of 480 nm, a Texas Red filter to detect RFP, dsRed, and mRuby2 signals at an emission of 568 nm, and a Quad filter to measure DAPI signal at emission of 451 nm and 647 nm to measure signal to Nhe6 antibody conjugated with Alexa 647. Aquiring the images used NIS Elements AR V4.1 software (Nikon Canada, Mississauga, ON, Canada).

Fixed neurons were imaged on a Leica SP2 point scanner confocal microscope with a 63X HCX Plan Apo oil immersion objective with an XY resolution at 148 nm and a Z resolution at 0.592 μm with a step size of 0.2 μm going 2 μm above and below the plane using Leica Confocal Software. A blue Argon 488 nm laser was used for detection of eGFP signal, a green Helium Neon 543 nm laser was used for detection of mRuby2 and Alexa 568, and a red Helium Neon 633 nm laser used to detect Alexa 647.

Colocalization in HeLa cells was determined by using object-based colocalization as previously described (Bayer et al., 2006) using the sliding threshold plugin for ImageJ with modifications (source code written by Gabriel Lapointe). Parameters included background-correction and the nucleus masked out via DIC and DAPI stain. A sliding threshold ranging from the minimum to maximum

values in increments of 50 intensity units was applied. To define an endosome, two criteria were used: a pixel area ranging from 0.4-5 μm^2 and shape that had a circularity of 0.7-1. Averages and SEM were calculated using Microsoft Excel v.14.0.2 (Microsoft Corporation, Redmond, WA, USA). Graphs were plotted using Kaleida Graph v.4.0 software (Synergy Software, Reading, PA, USA).

Videos of live neurons were recorded using a Nikon laser/sweptfield inverted microscope combined with LED-based epifluorescence using an iXon camera with a 100X oil objective. The microscope was set using a Quad filter; laser power settings set at the following: 488 nm – 15%, 561 nm – 15%, and 633 nm at 75%; at an exposure of 80 ms and EM gain of 300. The acquisition settings included 1 position with an XY resolution at 160 nm, Z resolution at step size 500 nm and thickness 3 μm, and (T) at 5 sec for duration of 10-30 minutes.

Images were processed using FIJI/ImageJ (downloaded from http://rsbweb.nih.gov/ij/) with brightness, contrast, windows, and levels adjusted. For neurons, a mask was created from the transfection of a cytoplasmic fill, when applicable and a subsequent outline was then created in FIJI/ImageJ using a threshold and then manually adjusted. Images were finally adjusted and arranged using Adobe Illustrator CS5 (Adobe System, San Jose, CA, USA).

2.5 Cloning

Human NHE6 cDNA and Mouse NHE9 cDNA were cloned previously (Brett et al., 2002 and Hill et al., 2006 respectively) with an enhanced Green Fluorescent Protein (GFP) epitope tag. The NHE9 construct expressing mRuby2 was produced by amplifying the mRuby coding sequence by polymerase chain reaction (PCR)

containing *EcoRI* and *XbaI* restriction sites using the pcDNA3 mRuby2 vector (Addgene, Cambridge, MA, USA) as a template. Cycling conditions were 98°C for 30 s; 30 cycles of 98°C for 10 s, 65°C for 30 s, 72°C for 60 s; and a final 10 min extension at 72°C. The product was amplified using Phusion HF DNA polymerase (New England Biolabs, Ipswich, MA, USA). The product was then gel purified (Qiagen, QIAquick gel extraction kit) to avoid contamination of an intact vector byproduct. The vector expressing NHE9 tagged with GFP was digested with *EcoRI* and *XbaI* and then gel purified in order to separate the DNA coding for GFP from the rest of the vector. The PCR product was then ligated into the linearized vector at *EcoRI* and *XbaI* sites in frame to make the NHE9-mRuby construct. The primers (Integrated DNA Technologies) used for this construct were as follows: cctgga*GAATTC*ATGGTGTCTAAGGGCGAAGA (forward) and tgcgca*TCTAGA*TTACTTGT ACAGCTCGTCCA (reverse). Italics represent the restriction sites (*EcoRI* and *XbaI* respectively). The lower cases indicate overhangs to increase binding efficiency of restriction enzymes and the upper cases signify the sequence targeting the coding sequence of mRuby2.

Plasmids coding for all Rab-GTPases epitope-tagged with GFP were a kind gift from Dr. John Presley (McGill University, Montréal, QC, Canada). The vectors expressing RFP-Rab5 and Rab9 and Rab11-dsRed were generous donations from Dr. Stéphane Lefrançois (Université de Montréal, Montréal, QC, Canada). Finally, the DNA constructs expressing human Nhe6-GFP and mouse Nhe9-GFP were provided by Dr. Alex Merz (University of Washington, Seattle, WA, USA).

3. Results

3.1 Nhe6 and Nhe9 are found on separate pools of Rab-positive endosomes in HeLa cells

In order to better understand the function of the mammalian orthologs of Nhx1, Nhe6 and Nhe9, my first aim was to determine which endocytic Rab-GTPases are found in the same compartments as these transporters. I first studied cell culture lines because multiple groups have shown that Nhe6 and Nhe9 are both found at endosomes within COS-7, CHO, OK-E3V, and HeLa cells (Brett et al., 2002; Nakamura et al., 2005; Ohgaki et al., 2008). Nhe6 colocalizes with early endosome markers, such as EEA1 (an effector of Rab5) and Rab 11, whereas Nhe9 is localized later in pathway than Nhe6, shown by timed internalization of transferrin, a marker of the endocytic pathway destined for degradation (Nakamura et al., 2005).

Rab-GTPases that function in the endocytic pathway include Rab5 at early endosomes, Rab11 at recycling endosomes, Rab7 at late endosomes, and Rab9 at the TGN (which is required for receptor recycling). Rab1 which localizes to the endoplasmic reticulum and *cis*-Golgi, was used as a negative control (Stenmark, 2009). As expected, endogenous Nhe6 showed no colocalization with over-expressed GFP-Rab1 or GFP-Rab7and Rab9-dsRed I the late endocytic pathway (Figure 1a). Rather, my results in HeLa cells confirm a previous report describing colocalization of Nhe6-GFP and Rab11 by immunofluorescence in cultured immortal opossum kidney (OK) cells, a model of polarized epithelial cells. Furthermore, I demonstrate that Nhe6-GFP colocalizes with RFP-Rab5 (Figure 1a). The degree of colocalization shows that Nhe6 localizes mostly at Rab5 and Rab11-positive

endosomes (Figure 1b), corresponding to early and recycling endosomes, respectively, confirming previous studies that suggest NHe6 is exclusively found in endosomes in the early part of the endocytic pathway.

Intracellular distribution of Nhe9 has not been studied in the past, in context to Rab-GTPases. A previous study has shown that Nhe9 colocalizes with transferrin later in the pathway than Nhe6 and showed a slight overlap with EEA1 and Nhe6 (Nakamura et al., 2005), indicating Nhe9 may have a role in recycling as well. Over-expression of Nhe9-mRuby is shown to mostly colocalizes with Rab7-positive endosomes (Figure 2a, 2b), consistent with studies performed in yeast. Interestingly, over-expression of Nhe9 showed similar levels of colocalization with both Rab11 and Rab5 (Figure 2b).

Nhe6 and Nhe9 are found on separate pools of endosomes (Figure1 and 2) with the exception of Rab11-positive endosomes where the early and late endocytic trafficking pathways diverge, confirming Rab11's localization to a recycling endosome. Although it is shown that Nhe9 shows a similar degree of colocalization with Rab5 as Nhe9 does with Rab11 (Figure 2b), it may have been due to the abundance of proximity Nhe9 had to Rab5 (Figure 2a).

3.2 Nhe6 and Nhe9 are found on separate pools of Rab-positive endosomes in hippocampal neurons

Because mutations in NHE6 and NHE9 cause neurodevelopmental disorders and both transporters are expressed in the brain (Lein et al., 2007) I repeated my

experiments using primary hippocampal neurons cultured from mice or rats to determine if Nhe6 and Nhe9 are expressed in neurons and if they are found in compartments containing Rab-GTPases.

Both endogenous and over-expression of Nhe6 showed a distribution throughout the soma and processes in distinct puncta in a similar fashion (Figure 3a). This confirms that hippocampal neurons endogenously express Nhe6. Since Nhe6 had similar distribution in both cases, the experiments were carried on using endogenous Nhe6 since it is more specific than over-expression.

Given that Nhe6 has never been studied in neurons, in respect to Rab-GTPases, it was integral to establish which compartments harbor Nhe6. Endogenous Nhe6 was immuno-fluorescently stained in neurons over-expressing GFP-Rab 7, 9, and 11 post-fixation after DIV 14-15. Distribution of Nhe6 among these Rab-GTPases was not entirely consistent with my previous results in HeLa cells, showing the most colocalization with Rab11 as well as with small subpopulations colocalizing with Rab 7 and Rab 9 (Figure 3b).

To date, Nhe9 has not been studied in cultured neurons at all, and therefore remains poorly understood. Over-expression of Nhe9 showed a similar distribution to Nhe6 (both endogenous and over-expression), shown as punctuate structures. However, although endogenous expression of Nhe9 showed signal throughout the soma and processes, the stain yielded excessive background in respect to the actual signal of interest and it could not be accurately distinguished between puncta (Figure 4a). Therefore, over-expression of Nhe9 was used. Nonetheless, this does

provide the first evidence that Nhe9 is endogenously expressed in hippocampal neurons.

When Nhe9 was over-expressed, it showed colocalization with all three Rab-GTPases (Figure 4b). Interestingly, Nhe9 colocalized with Rab9 in neurons but did not colocalize with Rab9 in HeLa cells. This data, in conjunction with the neuronal Nhe6 data, suggests that HeLa cells may not be a suitable model to study neurological diseases.

Finally, Nhe9 was over-expressed and counter-stained to endogenous and over-expression of Nhe6 to verify previous results stating that Nhe6 transiently colocalizes with Nhe9 (Nakamura et al., 2005) Two examples are shown (Figure 5) showing some colocalization of Nhe9 to both the endogenous staining and over-expression of Nhe6 in neurons. This may explain the overlap of both transporters with Rab11 in both HeLa cells and neurons and their possible role in recycling in the endocytic pathway. This is also confirms the previous study suggesting the Nhe6 and Nhe9 transiently colocalize with each other (Nakamura et al., 2005).

3.3 Nhe6 and Nhe9-positive endosomes are found within dendrites

Neurons have two main components: the axon, the pre-synaptic terminal which releases neurotransmitters, and the dendrites, which house the post-synapse full of neurotransmitter receptors. Prior to release, neurotransmitter-loaded vesicles fuse to the membrane are exocytosed into the synaptic cleft. Once bound to their respective receptors, they can be internalized and endocytosed for degradation or recycling back to the plasma membrane. Since Nhe6 and Nhe9 have been implicated in the endocytic pathway, experiments were then conducted to

determine if Nhe6 and Nhe9 are located within dendrites of neurons, counter-staining against PSD-95, a scaffolding protein at the post-syanptic density in dendritic spines of neurons.

Over-expression of Nhe6 showed to colocalize in a densely packed area, in what appears to a dendritic spine, with endogenous PSD-95 (Figure 6a) and endogenous staining of Nhe6 showed small overlap with endogenous PSD-95 (Figure 6b). Another group has reported similar findings for Nhe6 (Deane et al., 2013), showing Nhe6 to be recruited to dendritic spines following chemical induction of LTP. However, Nhe9 still remains largely uncharacterized, thus I decided to focus on this transporter for the remainder of my studies.

Nhe9 appeared to be juxtaposed to endogenous PSD-95 (Figure 6c). Although both did not colocalize with PSD-95, both Nhe6 and Nhe9 seem to be in dendrites of neurons. These findings further suggest that perhaps Nhe6 has an earlier role in endocytosis in neurons than Nhe9 does, whereas Nhe9 may have its role later in the pathway, as previously predicted.

3.4 Nhe9 is found on mobile compartments that transiently fuses to and from Rab-positive endosomes in hippocampal neurons

Both NHEs and Rab-GTPases have been implicated in membrane trafficking and fusion. Yeast *nhx1*Δ mutants yield trafficking defects such as increased cargo recycling and impaired late endosome-vacuole fusion *(*Bowers et al., 2000; Ali et al., 2004; Brett et al., 2005b). Although it was found that Nhe9 colocalizes, to some degree, with each Rab7, Rab9, and Rab11 (Figure 4b), it is still unclear whether

these proteins are natively at the same compartment, or whether two separately labeled compartments fuse together.

A still photo of a video shows Rab7-positve compartments and Nhe9-positive endosomes moving through the processes in neurons (refer to Supplemental video file 1), confirming that these individual compartments are, in fact, mobile throughout the cell (Figure 7a). Figure 7b is a zoomed time course showing an Nhe9-positive compartment (red) come together with a Rab7-positive endosome at the marked area (blue circle) at the 28s time point and remaining there until the 60s time point (refer to Supplemental video file 2) and then move away from each other. This overlap suggests a heterotypic fusion event between the two compartments. The data also shows what appears to be a homotypic fusion event between two different Rab7 compartments also shown at the 60s time point. Later shown, at the 91s time point, is what appears to be a Rab7-positive endosome undergoing a fission event from an Nhe9-positve compartment.

In Figure 8a, a snapshot from a video of a region of a neuron shows Rab9-positive and Nhe9-positve endosomes also moving through the processes (refer to Supplemental video file 3). Figure 8b shows a time course of Nhe9 moving through field, first appearing to come off a Rab9-positive endosome at the right at time point 0s where it then proceeds to come together with another endosome decorated with Rab9 at time point 135s, in which this new compartment stays in place for almost a minute when you happen to see what appears to be another fusion event at time point 180s. After the supposed fusion event, both compartments appear to move towards the left (refer to Supplemental video file 4). Noteworthy, the Rab9-positive

endosomes visible from 90s to the end of the video that do not undergo a fusion event, appear to remain static throughout the duration of the video. This may imply a potential role for Nhe9 in potentiating Rab9-containing endosomes to become mobile.

To verify whether Nhe9-positive endosomes are involved in the recycling endocytic pathway in addition to the late aspects of the endocytic pathway, Nhe9 was finally looked at in regards to Rab11. A photographic representation of a video showing mobility of Nhe9 and Rab11 in the processes is portrayed in Figure 9a (refer to Supplemental video file 5). A time course is also shown in Figure 9b showing Nhe9 and Rab11-positive compartments which appear to be tethered or docked to each other and moving together. They then separate from each other at the 60s time point, and then appear to undergo a fusion event at the 120s time point, then appear to undergo fission 20 seconds later.

Figure 1: Intracellular distribution of Nhe6 in HeLa cells.

(a) Fluorescence micrographs of cultured HeLa cells over-expressing GFP-Rab1 and Rab7 and stained with an antibody to Nhe6 and DAPI (top) and over-expressing RFP-tagged Rab5, dsRed-tagged Rab9 and Rab11, and Nhe6-GFP stained with DAPI (bottom). Panels at the far right are zoomed in on the box drawn in the Merge column. Blue arrowheads indicate overlapping puncta. Bar, 20 μm. (b) Bar graph representing the analysis of percentage of colocalization of Nhe6 with Rab-GTPases with SEM error bars. For each condition, 3-6 coverslips were prepared whereby over 10 cells were imaged.

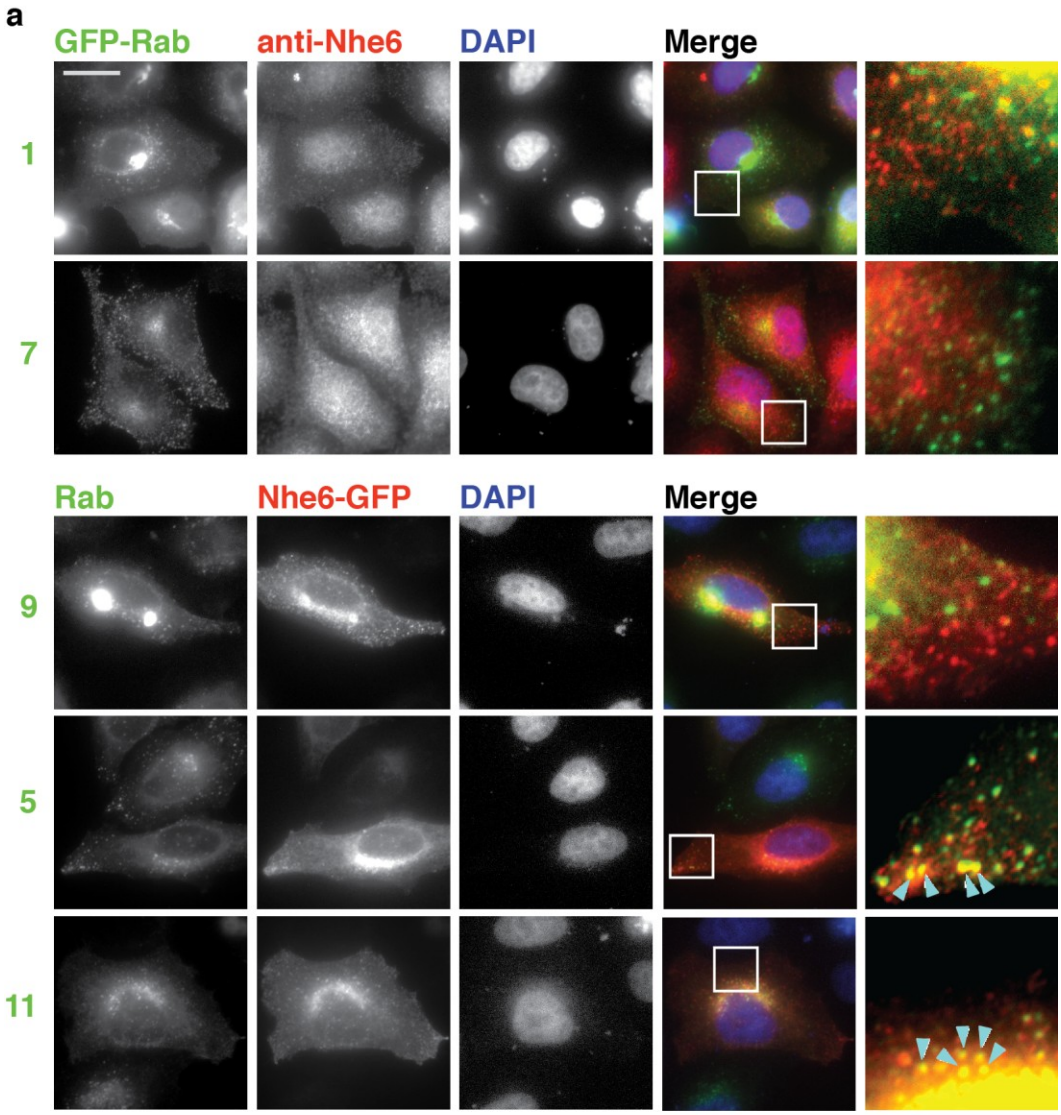
a
GFP-Rab
anti-Nhe6
DAPI
Merge
1
7
Rab
Nhe6-GFP
DAPI
Merge
9
5
11

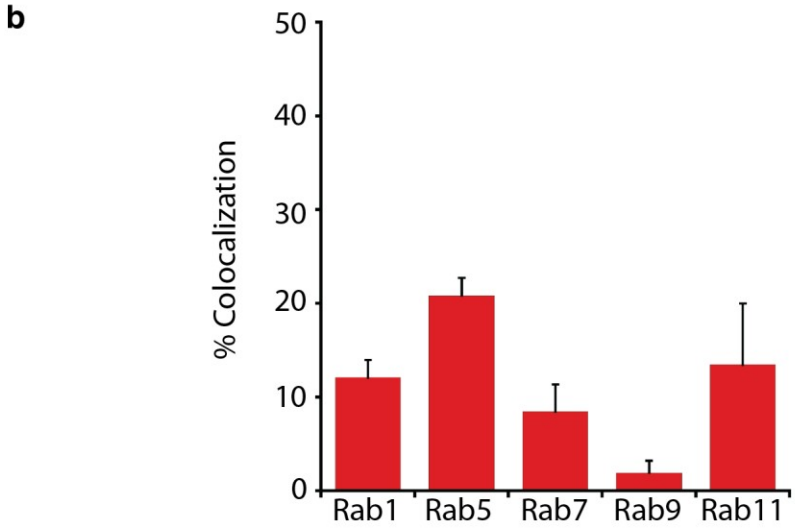
b
% Colocalization
50
40
30
20
10
0
Rab1
Rab5
Rab7
Rab9
Rab11

Figure 2: Intracellular distribution of Nhe9 in HeLa cells.

(a) Fluorescence micrographs of cultured HeLa cells over-expressing GFP-Rab1 and Rab7, Rab5-RFP, Rab9 and Rab11-dsRed, Nhe9-mRuby2 and staining with DAPI. Panels at the far right are zoomed in on the box drawn in the Merge column. Blue arrowheads indicate overlapping puncta. Bar, 20 μm. (b) Bar graph representing the analysis of percentage of colocalization of Nhe9 with Rab-GTPases with SEM error bars. For each condition, 3-6 coverslips were prepared whereby over 10 cells were imaged.

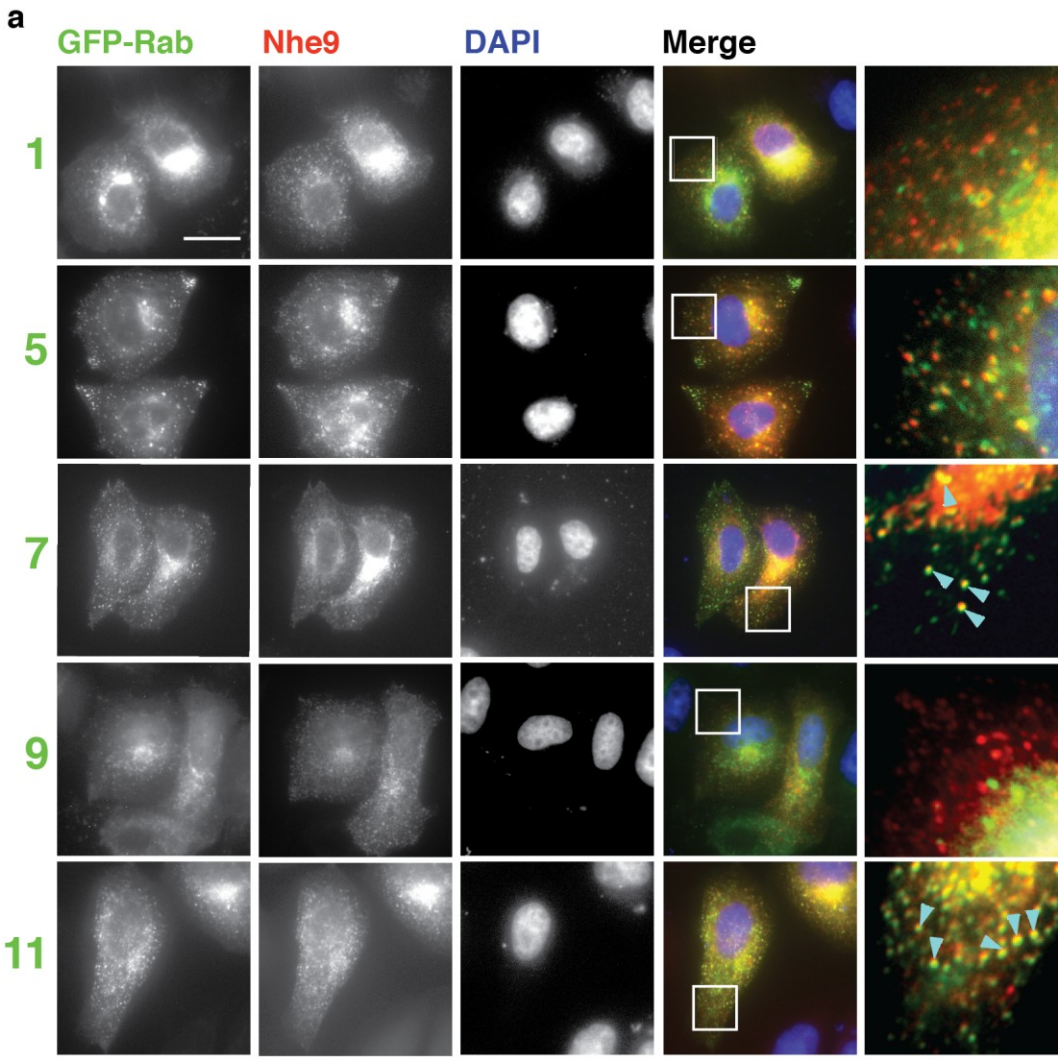
a
GFP-Rab
Nhe9
DAPI
Merge
1
5
7
9
11

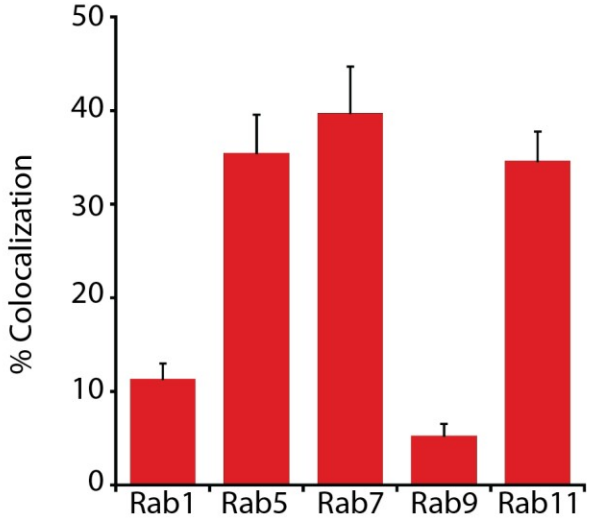
% Colocalization
50
40
30
20
10
0
Rab1
Rab5
Rab7
Rab9
Rab11

Figure 3: Intracellular distribution of Nhe6 in hippocampal neurons.

(a) Fluorescence micrographs showing examples of cultured rat hippocampal neurons and glia cells stained with antibody against Nhe6 (left panel) and transiently over-expressing NHE6 from a plasmid (right panel). Bar, 2 μm. (b) Fluorescence micrographs showing rat hippocampal neurons over-expressing a Rab-GTPase and mRuby2 from a plasmid and stained with antibody against Nhe6. Bar, 20 μm. Panels underneath the whole cell view are zoomed in on the box drawn in the Merge column. Blue arrowheads indicate overlapping puncta. Bar, 2 μm. For each condition, 3-6 separate coverslips were prepared whereby over 5 cells were imaged.

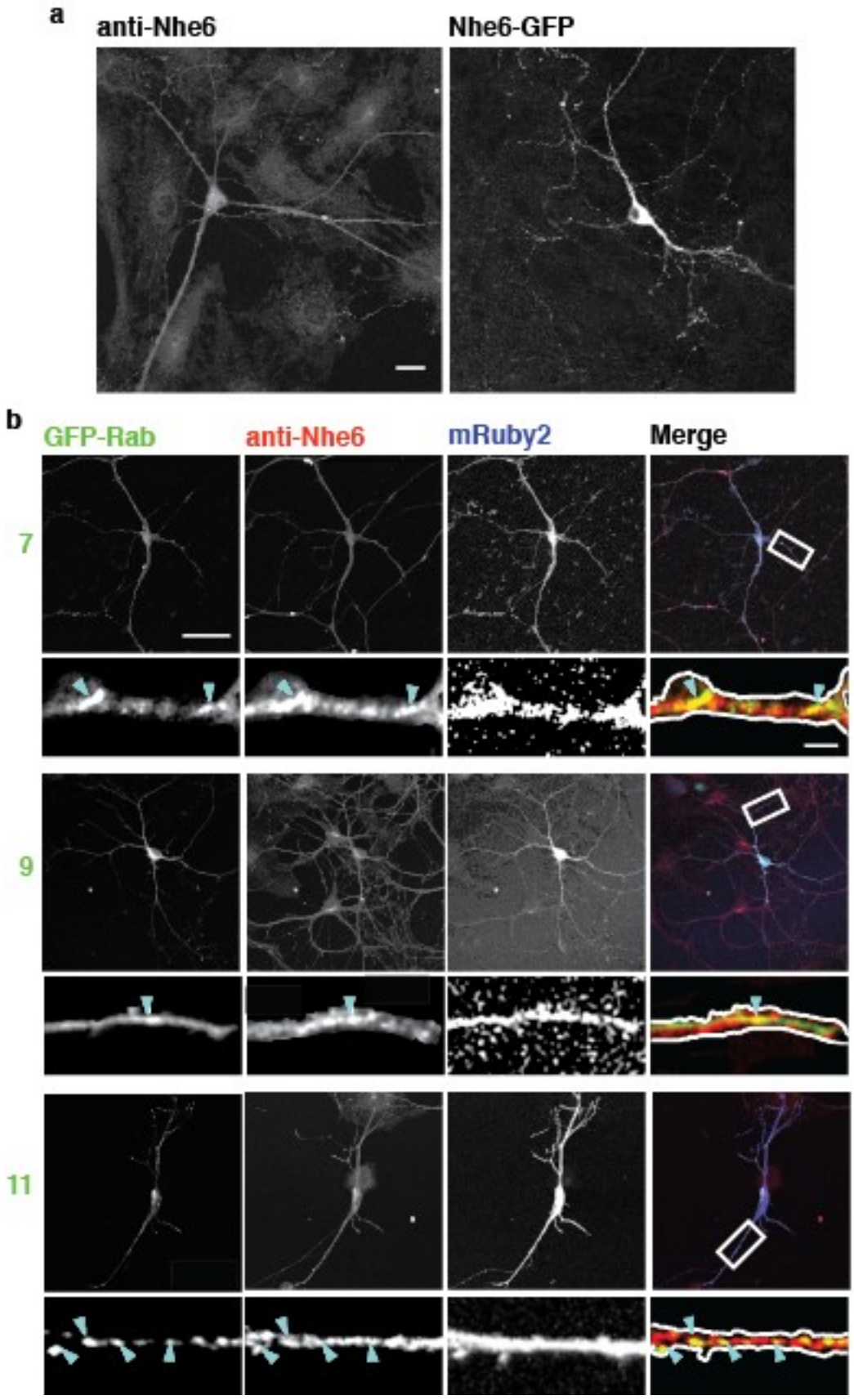
a
anti-Nhe6
Nhe6-GFP
b
GFP-Rab
anti-Nhe6
mRuby2
Merge
7
9
11

Figure 4: Intracellular distribution of Nhe9 in hippocampal neurons.

(a) Fluorescence micrographs showing examples of cultured mouse hippocampal neurons and glia cells stained with antibody against Nhe9 (left panel) and transiently over-expressing NHE9 from a plasmid (right panel). Bar, and 20 μm respectively. (b) Fluorescence micrographs showing mouse hippocampal neurons over-expressing NHE9, a Rab-GTPase, and iRFP from a plasmid. Bar, 20 μm. Panels underneath the whole cell view are zoomed in on the box drawn in the Merge column. Blue arrowheads indicate overlapping puncta. Bar, 5 μm. For each condition, 3-6 separate coverslips were prepared whereby over 5 cells were imaged.

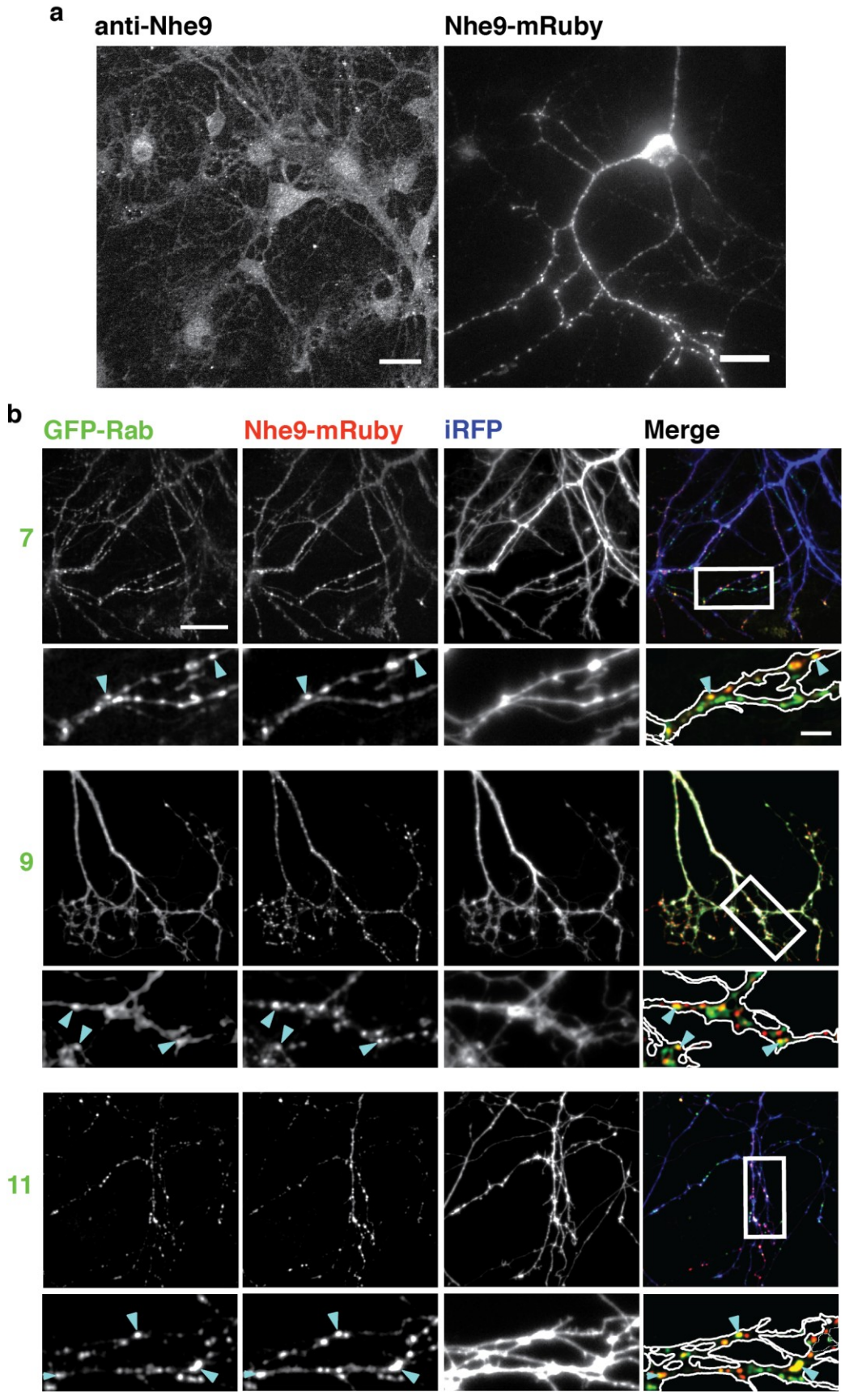
a
anti-Nhe9
Nhe9-mRuby
b
GFP-Rab
Nhe9-mRuby
iRFP
Merge
7
9
11

Figure 5: Distribution of Nhe6 and Nhe9 in hippocampal neurons.

(a) Fluorescence micrographs showing cultured rat hippocampal neurons over-expressing NHE9 and mRuby2 from a plasmid and stained with an antibody to Nhe6 (top). Bar, 20 μm. Panels underneath the whole cell view are zoomed in on the box drawn in the Merge column. Blue arrowheads indicate overlapping puncta. Bar, 2 μm. (b) Fluorescence micrographs showing cultured mouse hippocampal neurons over-expressing NHE6, NHE9, and. Scale bar set to 20 μm. Panels underneath the whole cell view are zoomed in on the box drawn in the Merge column. Blue arrowheads indicate overlapping puncta. Scale bar set to 5 μm. For each condition, 3-6 separate coverslips were prepared whereby over 5 cells were imaged.

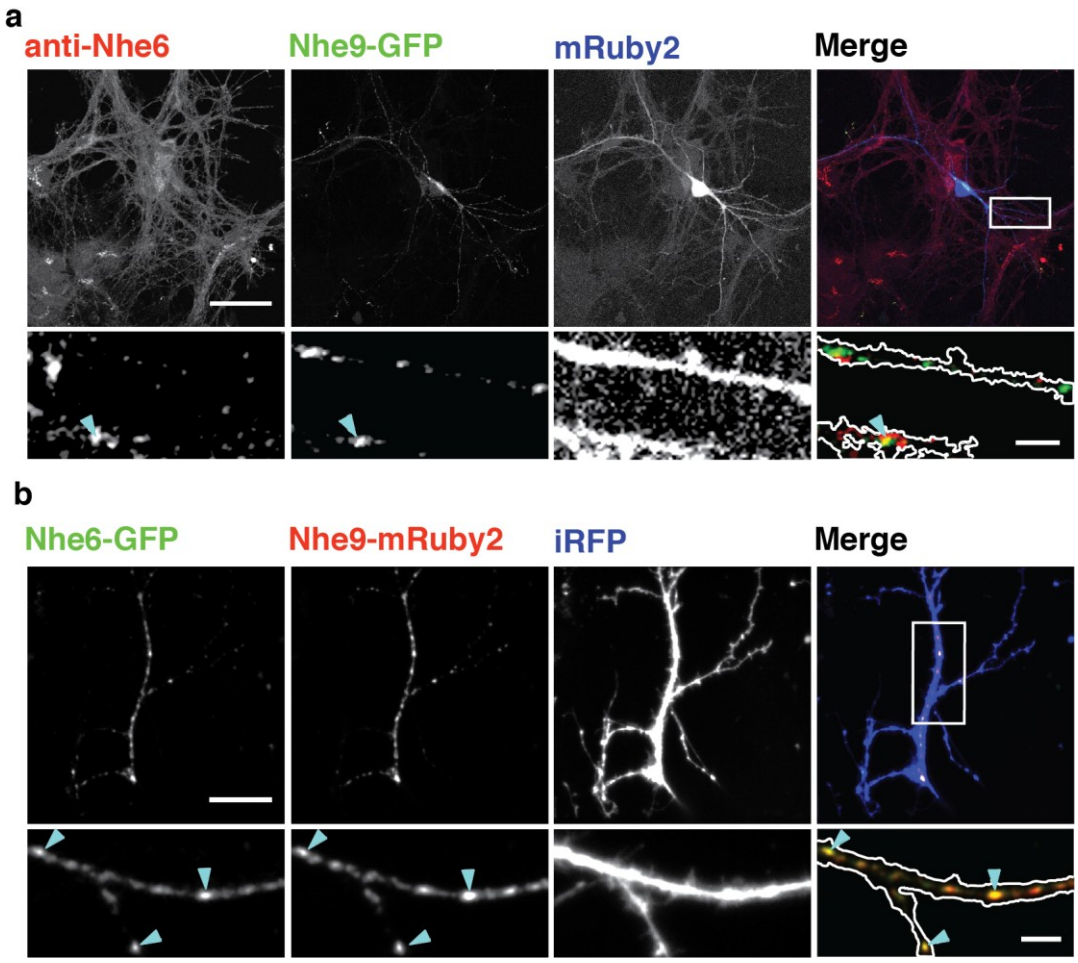
a
anti-Nhe6
Nhe9-GFP
mRuby2
Merge
b
Nhe6-GFP
Nhe9-mRuby2
iRFP
Merge

Figure 6: Nhe6 and Nhe9 are in endosomes in neuronal dendrites

(a) Fluorescence micrographs of cultured rat hippocampal neurons over-expressing NHE6 from a plasmid and stained with an antibody to PSD-95. Bar, 2 μm. Panels underneath the whole cell view are zoomed in on the box drawn in the Merge column. Blue arrowheads indicate overlapping puncta. Bar, 2 μm. (b) Fluorescence micrographs of cultured rat hippocampal neurons cultured and stained with antibodies to Nhe6 and PSD-95. Bar, 2 μm. Panels underneath the whole cell view are zoomed in on the box drawn in the Merge column. Blue arrowheads indicate overlapping puncta. Bar, 2 μm. (c) Fluorescence micrographs of cultured rat hippocampal neurons over-expressing NHE9 from a plasmid and stained with an antibody to PSD-95. Bar, 20 μm. Panels underneath the whole cell view are zoomed in on the box drawn in the Merge column. Blue arrowheads indicate overlapping puncta. Bar, 5 μm.

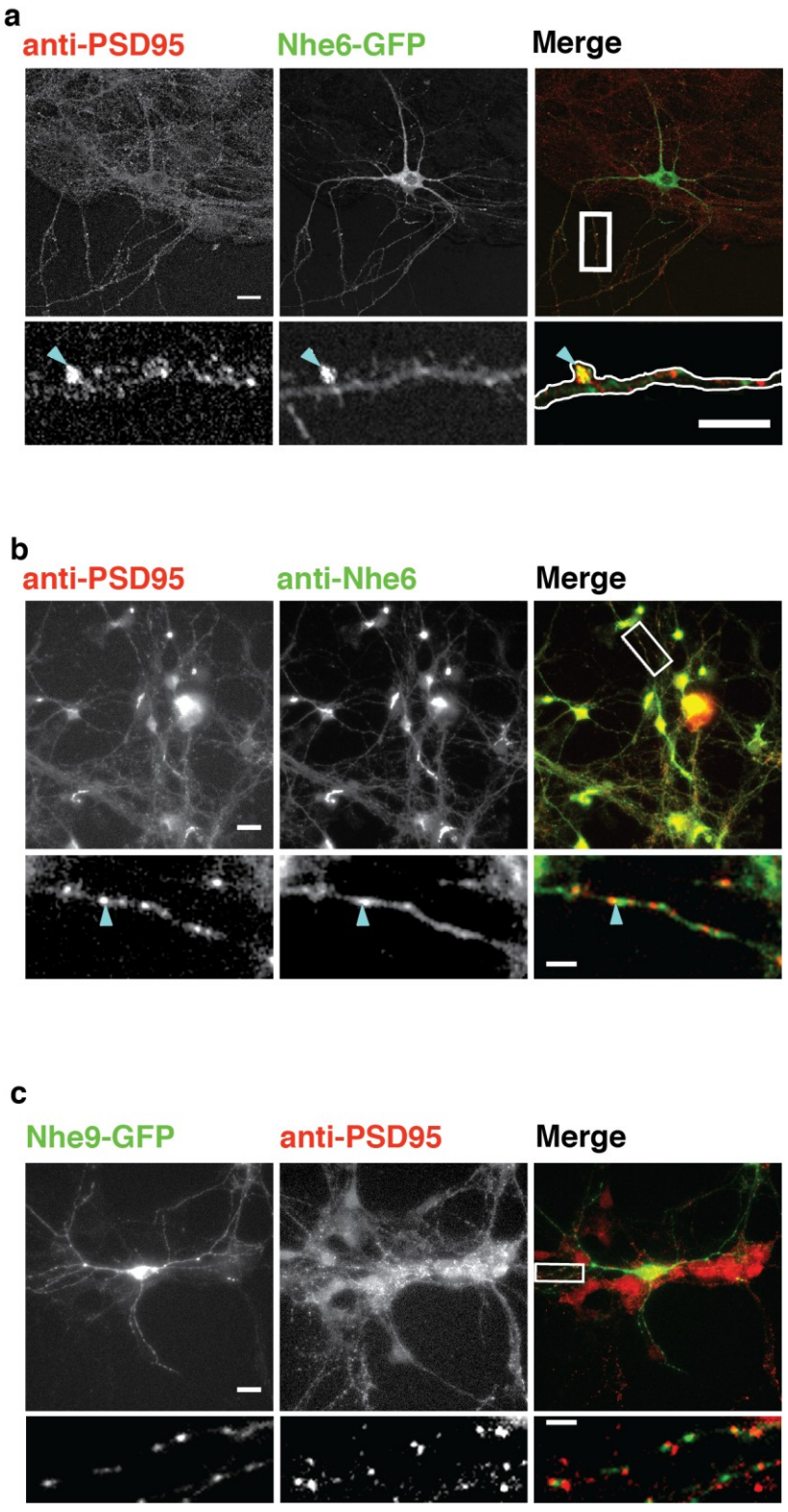
a
anti-PSD95
Nhe6-GFP
Merge
b
anti-PSD95
anti-Nhe6
Merge
c
Nhe9-GFP
anti-PSD95
Merge

Figure 7: Nhe9 is found on mobile compartments that transiently fuse to Rab7-positive compartments.

(a) Video depiction of cultured mouse hippocampal neurons over-expressing Rab7, NHE9, and iRFP and viewed live. Scale bar is set to 20 μm. (b) Zoomed video time course showing a Rab7-positive endosome (green) moving towards an Nhe9-positive compartment (red). Scale bar set to 2 μm.

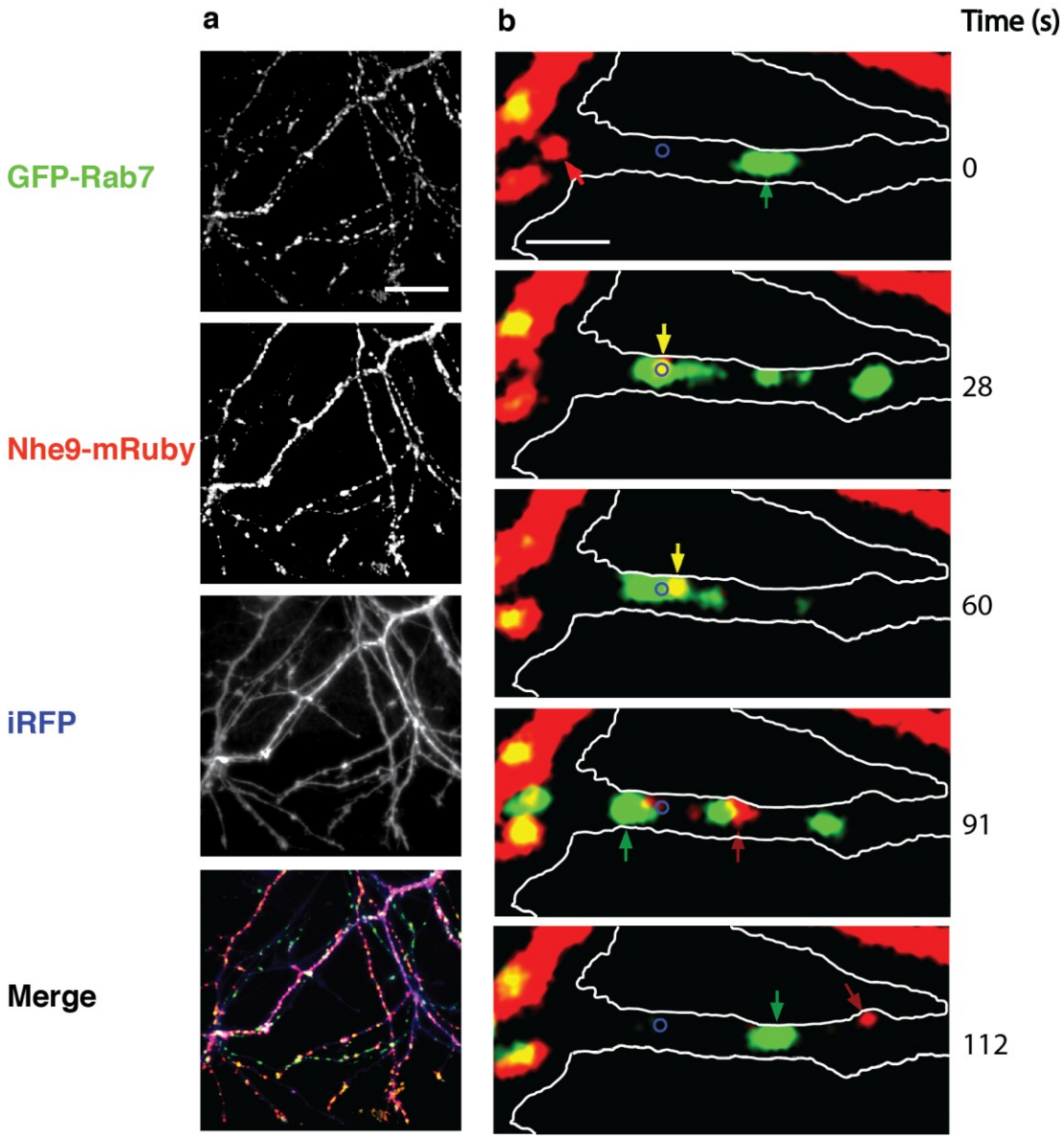
a
b
Time (s)
GFP-Rab7
Nhe9-mRuby
iRFP
Merge
0
28
60
91
112

Figure 8: Nhe9 is found on mobile compartments that transiently fuse to Rab9-positive compartments.

(a) Video of mouse hippocampal neurons over-expressing GFP-Rab9, Nhe9-mRuby2, and iRFP and viewed live under a fluorescent microscope. Scale bar is set to 20 μm. (b) Zoomed video time course showing an Nhe9-positive compartment (red) moving towards a Rab9-positive endsome (green) and the . Scale bar set to 2 μm.

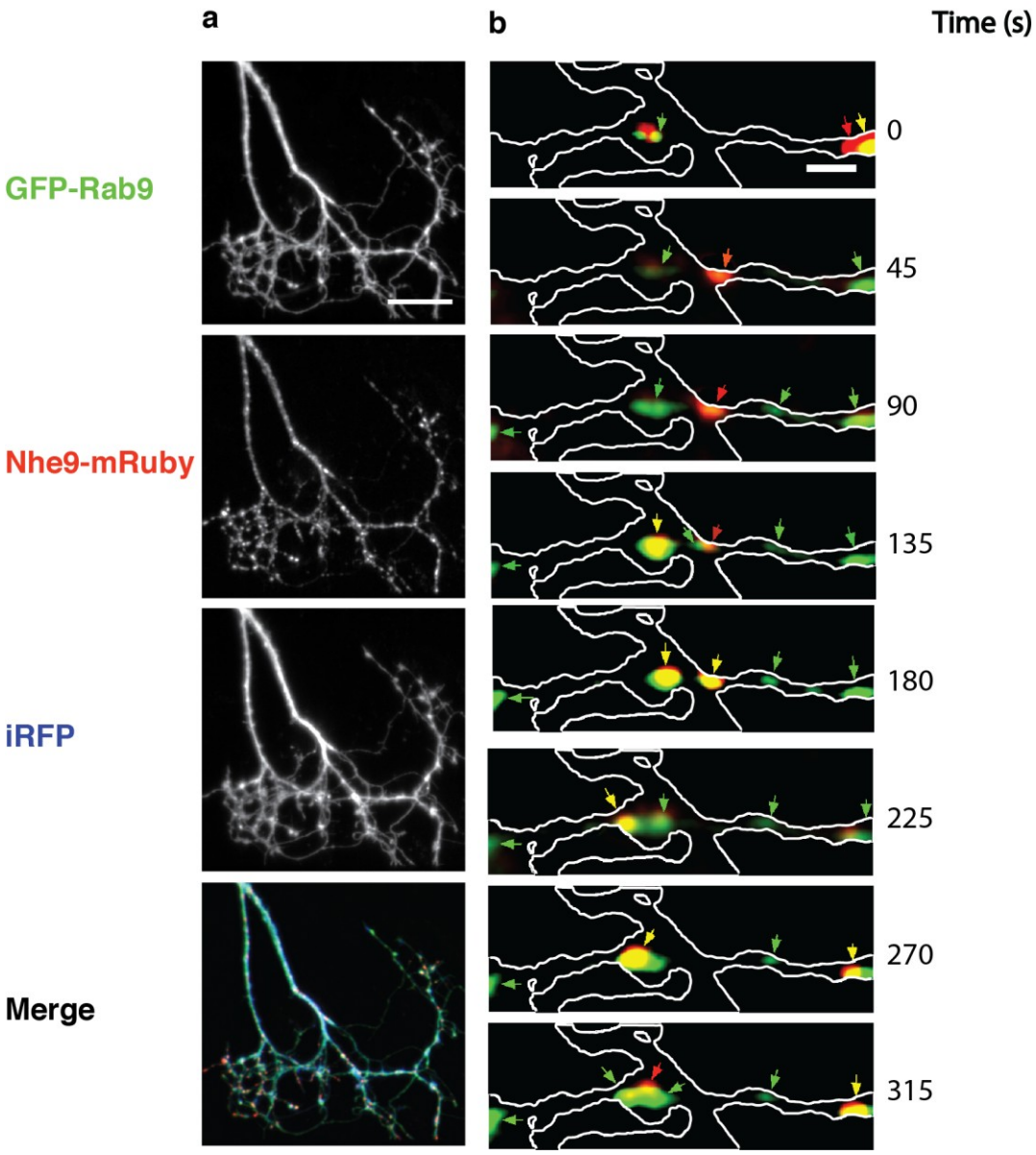
a
b
Time (s)
GFP-Rab9
Nhe9-mRuby
iRFP
Merge
0
45
90
135
180
225
270
315

Figure 9: Nhe9 is found on mobile compartments that transiently fuse to Rab11-positive compartments.

(a) Video of mouse hippocampal neurons over-expressing GFP-Rab11, Nhe9-mRuby2, and iRFP and viewed live under a fluorescent microscope. Scale bar is set to 20 μm. (b) Zoomed video time course showing a Rab11-positive endosome (green) moving with an Nhe9-positive compartment (red), separating, then appearing to fuse again. Scale bar set to 2 μm.

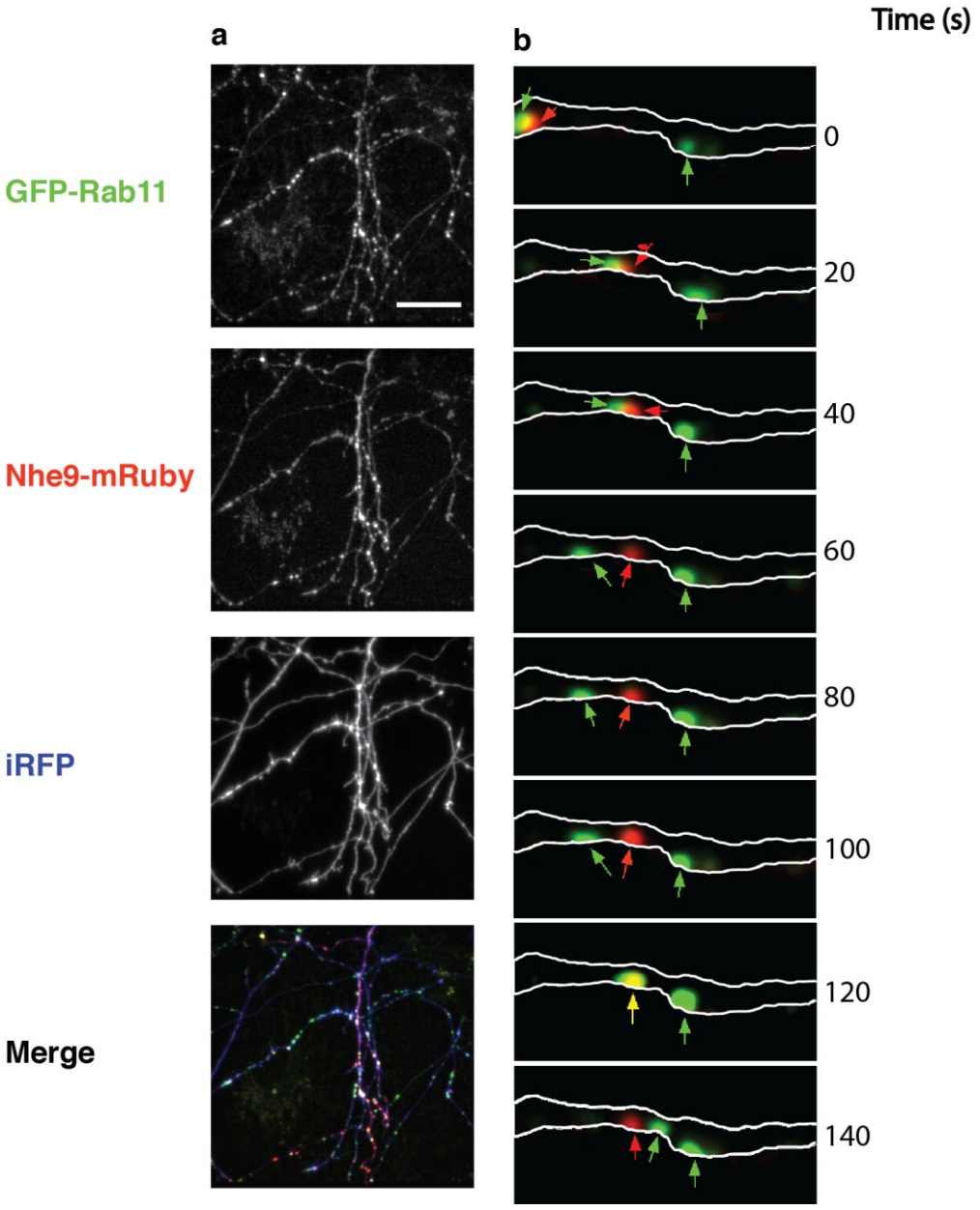
a
b
Time (s)
GFP-Rab11
Nhe9-mRuby
iRFP
Merge
0
20
40
60
80
100
120
140

4. Discussion

Recent studies have implicated mutations in both human NHE6 and NHE9 in neurological disorders such as ASDs, autism, and Christianson Syndrome in which patients may present with hyperactivity, severe mental retardation, epilepsy, and ataxia (Gilfillan et al., 2008; Morrow et al., 2008; Toro et al., 2010). It has also been shown that NHE6-knockout mice exhibit cerebellar atrophy and Purkinje cell loss (Strømme et al., 2011). In spite of these dramatic disorders with severe phenotypes, little is known about both NHE6 and NHE9. In this thesis, I show that Nhe6 and Nhe9 are localized to recycling and late endosomes, respectively; that both Nhe6 and Nhe9 are found in dendrites of neurons; and that Nhe9-positive endosomes appear to fuse with Rab-GTPase-positive compartments.

The specific sub-cellular localization of each transporter may have immense effects in regards to different neurological disorders. With the combined data of showing Nhe6 in mostly Rab11-postive compartments (Figure 1a) (indicative of recycling endosomes), Nhe6 colocalizing with PSD-95 (Figure 6a), and the previous data showing the recruitment of Nhe6 in dendritic spines following the induction of chemical LTP (Deane et al., 2013), it suggests that Nhe6 may play a role in synaptic plasticity and neurotransmitter receptor recycling. The colocalization of Nhe6 with Rab5-positive endosomes in HeLa cells (Figure 1a) also suggests a role for Nhe6 early in the endocytic pathway. The high degree of colocalization of Nhe9 with Rab7 and Rab11 in HeLa cells (Figure 2b) suggest its role later in the endocytic pathway, confirming previous results (Nakamura et al., 2005). The high degree of colocalization of Nhe9 with Rab5 was curious, as Rab5 functions at early endosomes

(Stenmark, 2009). However, Stenmark shows that Rab5-positive endosomes are in close proximity to Rab7 and Rab9-containing late endosomes as well as being located at early phagosomes, which fuse to Rab7-decorated late phagosomes. Live cell imaging of these two constructs could confirm whether or not they seem to fuse to one another.

Although Nhe6 seemed to colocalize mostly with Rab11 in hippocampal neurons, there was still a small degree of colocalization with late endosome markers Rab7 and Rab9. This can also be explained by the fact that recycling endosomes are at the junction between early and late endocytosis, and the recycling endosome can go either way – anterogradely towards the lysosome or retrogradely back to the TGN or surface.

Of high interest, was the observation that a Rab9-positive endosome remained static, until an Nhe9-decorated compartment appeared to fuse with it. Rab9 is a late endosomal GTPase that mediates trafficking from late endosomes to the TGN (Stenmark, 2009) and perhaps Nhe9 may influence Rab9's ability to shuttle between the TGN and late endosomes where they can fuse to lysosomes for degradation. Although the data indicates a possible fusion event (Figures 7b, 8b, 9b) between Nhe9-positive compartments and Rab-labeled endosomes, perhaps a more definitive analysis would be to use fluorescence resonance energy transfer (FRET), which only occurs when the molecules of interest are in very close proximity to each other.

My work sets up the basis for future experiments which can help determine whether AMPA or NMDA receptor subunits (or both?) get trafficked through Nhe6

and/or Nhe9-positive endosomes. In conjunction with these experiments, an NHE6-knockout mouse model or the use of siRNA could be used to determine the effect of neurotransmitter receptor recycling. I predict that a loss of function in Nhe6 and Nhe9 would affect receptor degradation and increase recycling of receptors to the plasma membrane. Similar to NHX1Δ yeast, these mutants presented trafficking defects with enlarged, aberrant endosomes, increased recycling of surface cargo back to the surface, and hyperacidic compartments (Ali et al., 2004; Brett et al., 2005b). SinceNHE6 and NHE9 are bona fide orthologs of NHX1 (Hill et al., 2006), I expect similar results in respect to all three phenotypes observed in yeast.

This phenomenon could explain some of the phenotypes underlying neurological disorders such as Christianson Syndrome, including epilepsy and hyperactivity. With increased expression of neurotransmitter receptors, more neurotransmitter has the potential to bind. An increase in activation of AMPA an NMDA receptors (both glutamate receptors) increases excitatory responses and too much of or an uncontrolled increase could explain the over-excitability some patients may present.

With the Nhe9 data suggesting its localization later in the endocytic pathway, with its association with Rab9 and Rab7 in neurons, as well as its transient colocalization with Rab11, its role in neurological diseases could be explained by its role in degradation and recycling of neurotransmitter receptors due to failed delivery to the lysosome. Of the four intracellular NHEs, Nhe9 is most similar in amino acid sequence to yeast Nhx1. It has recently been shown that Nhx1 colocalizes 100% with Vps10 (Kojima et al., 2012). The human ortholog of Vps10,

Sortilin, which is vital for trafficking of proteins from the TGN to the lysosome and has been implicated in Alzheimer's Disease and memory retention in Alzheimer's patients (Lefrancois et al., 2003; Rogaeva et al., 2007; Reitz et al., 2011). Sortilin has also been shown to be expressed in neurons and regulated by synaptic activity by facilitating rapid endocytosis (Hermey et al., 2001, 2004). Future experiments will involve determining if Nhe9 localizes with Sortilin at the TGN. If Nhe9 does, in fact, colocalize with Sortilin, I predict that a loss of function in Nhe9 will affect the ability for the cell to properly internalize and send cargo to the lysosome for degradation. Thus, I predict for the entire trafficking system to be delayed with a toxic buildup of proteins not being degraded.

As an alternative to transferrin, nanocarrier particles mark other endocytic pathways, such as macropinocytosis versus receptor-mediated endocytosis. Nanocarriers are made of various polymer coats that encapsulate drugs meant for cellular delivery, without exposure to the extracellular environment. Nanocarriers are internalized into endosomes with a low pH environment that allows depolymerization of the coat, releasing the drug. Thus, nanocarriers may be a future treatment option for Nhe6 and Nhe9-related disorders because they can target a specific cell population based on surface epitopes, and are readily internalized into endosomal compartments. A possible future treatment to look into is to load a weak base into a nanocarrier. Previous studies have shown that NHX1Δ yeast showed a hyperacidic lumen and the subsequent phenotypes associated with NHX1Δ being rescued with the treatment of a weak base (Brett et al., 2005b) and that over-expression of Nhe9 caused an increase of pH in COS-7 cells (Nakamura et al., 2005),

indicating that the loss of function of Nhe9 would decrease pH. Future experiments will involve nanocarriers with a weak base and observe any endocytic defects caused by loss of function of Nhe6 or Nhe9.

5. References

Ali, R., C.L. Brett, S. Mukherjee, and R. Rao. 2004. Inhibition of sodium/proton exchange by a Rab-GTPase-activating protein regulates endosomal traffic in yeast. *The Journal of biological chemistry*. 279:4498–506.

Balderhaar, H.J.K., H. Arlt, C. Ostrowicz, C. Bröcker, F. Sündermann, R. Brandt, M. Babst, and C. Ungermann. 2010. The Rab GTPase Ypt7 is linked to retromer-mediated receptor recycling and fusion at the yeast late endosome. *Journal of cell science*. 123:4085–94.

Bayer, K.U., E. LeBel, G.L. McDonald, H. O'Leary, H. Schulman, and P. De Koninck. 2006. Transition from reversible to persistent binding of CaMKII to postsynaptic sites and NR2B. *The Journal of neuroscience : the official journal of the Society for Neuroscience*. 26:1164–74.

Bos, J.L., H. Rehmann, and A. Wittinghofer. 2007. GEFs and GAPs: critical elements in the control of small G proteins. *Cell*. 129:865–77.

Bowers, K., B.P. Levi, F.I. Patel, and T.H. Stevens. 2000. The sodium/proton exchanger Nhx1p is required for endosomal protein trafficking in the yeast Saccharomyces cerevisiae. *Molecular biology of the cell*. 11:4277–94.

Brett, C.L., M. Donowitz, and R. Rao. 2005a. Evolutionary origins of eukaryotic sodium/proton exchangers. *American journal of physiology. Cell physiology*. 288:C223–39.

Brett, C.L., R.L. Plemel, B.T. Lobingier, B.T. Lobinger, M. Vignali, S. Fields, and A.J. Merz. 2008. Efficient termination of vacuolar Rab GTPase signaling requires coordinated action by a GAP and a protein kinase. *The Journal of cell biology*. 182:1141–51.

Brett, C.L., D.N. Tukaye, S. Mukherjee, and R. Rao. 2005b. The yeast endosomal Na+K+/H+ exchanger Nhx1 regulates cellular pH to control vesicle trafficking. *Molecular biology of the cell*. 16:1396–405.

Brett, C.L., Y. Wei, M. Donowitz, and R. Rao. 2002. Human Na(+)/H(+) exchanger isoform 6 is found in recycling endosomes of cells, not in mitochondria. *American journal of physiology. Cell physiology*. 282:C1031–41.

Cox, G.A., C.M. Lutz, C.L. Yang, D. Biemesderfer, R.T. Bronson, A. Fu, P.S. Aronson, J.L. Noebels, and W.N. Frankel. 1997. Sodium/hydrogen exchanger gene defect in slow-wave epilepsy mutant mice. *Cell*. 91:139–48.

Deane, E.C., A.E. Ilie, S. Sizdahkhani, M. Das Gupta, J. Orlowski, and R.A. McKinney. 2013. Enhanced recruitment of endosomal Na+/H+ exchanger NHE6 into Dendritic spines of hippocampal pyramidal neurons during NMDA receptor-dependent long-term potentiation. *The Journal of neuroscience : the official journal of the Society for Neuroscience*. 33:595–610.

Denker, S.P., and D.L. Barber. 2002. Cell migration requires both ion translocation and cytoskeletal anchoring by the Na-H exchanger NHE1. *The Journal of cell biology*. 159:1087–96.

Ebert, D.H., and M.E. Greenberg. 2013. Activity-dependent neuronal signalling and autism spectrum disorder. *Nature*. 493:327–37.

Epp, N., R. Rethmeier, L. Krämer, and C. Ungermann. 2011. Membrane dynamics and fusion at late endosomes and vacuoles--Rab regulation, multisubunit tethering complexes and SNAREs. *European journal of cell biology*. 90:779–85.

Gilfillan, G.D., K.K. Selmer, I. Roxrud, R. Smith, M. Kyllerman, K. Eiklid, M. Kroken, M. Mattingsdal, T. Egeland, H. Stenmark, H. Sjøholm, A. Server, L. Samuelsson, A. Christianson, P. Tarpey, A. Whibley, M.R. Stratton, P.A. Futreal, J. Teague, S. Edkins, J. Gecz, G. Turner, F.L. Raymond, C. Schwartz, R.E. Stevenson, D.E. Undlien, and P. Strømme. 2008. SLC9A6 mutations cause X-linked mental retardation, microcephaly, epilepsy, and ataxia, a phenotype mimicking Angelman syndrome. *American journal of human genetics*. 82:1003–10.

Hermey, G., N. Plath, C.A. Hübner, D. Kuhl, H.C. Schaller, and I. Hermans-Borgmeyer. 2004. The three sorCS genes are differentially expressed and regulated by synaptic activity. *Journal of neurochemistry*. 88:1470–6.

Hermey, G., I.B. Riedel, M. Rezgaoui, U.B. Westergaard, C. Schaller, and I. Hermans-Borgmeyer. 2001. SorCS1, a member of the novel sorting receptor family, is localized in somata and dendrites of neurons throughout the murine brain. *Neuroscience letters*. 313:83–7.

Hill, J.K., C.L. Brett, A. Chyou, L.M. Kallay, M. Sakaguchi, R. Rao, and P.G. Gillespie. 2006. Vestibular hair bundles control pH with (Na+, K+)/H+ exchangers NHE6 and NHE9. *The Journal of neuroscience : the official journal of the Society for Neuroscience*. 26:9944–55.

Kennedy, M.J., and M.D. Ehlers. 2006. Organelles and trafficking machinery for postsynaptic plasticity. *Annual review of neuroscience*. 29:325–62. doi:10.1146/annurev.neuro.29.051605.112808.

Kojima, A., J.Y. Toshima, C. Kanno, C. Kawata, and J. Toshima. 2012. Localization and functional requirement of yeast Na+/H+ exchanger, Nhx1p, in the endocytic and protein recycling pathway. *Biochimica et biophysica acta*. 1823:534–43.

Lefrancois, S., J. Zeng, A.J. Hassan, M. Canuel, and C.R. Morales. 2003. The lysosomal trafficking of sphingolipid activator proteins (SAPs) is mediated by sortilin. *The EMBO journal*. 22:6430–7.

Lein, E.S., M.J. Hawrylycz, N. Ao, M. Ayres, A. Bensinger, A. Bernard, A.F. Boe, M.S. Boguski, K.S. Brockway, E.J. Byrnes, L. Chen, L. Chen, T.-M. Chen, M.C. Chin, J. Chong, B.E. Crook, A. Czaplinska, C.N. Dang, S. Datta, N.R. Dee, A.L. Desaki, T. Desta, E. Diep, T.A. Dolbeare, M.J. Donelan, H.-W. Dong, J.G. Dougherty, B.J. Duncan, A.J. Ebbert, G. Eichele, L.K. Estin, C. Faber, B.A. Facer, R. Fields, S.R. Fischer, T.P. Fliss, C. Frensley, S.N. Gates, K.J. Glattfelder, K.R. Halverson, M.R. Hart, J.G. Hohmann, M.P. Howell, D.P. Jeung, R.A. Johnson, P.T. Karr, R. Kawal, J.M. Kidney, R.H. Knapik, C.L. Kuan, J.H. Lake, A.R. Laramee, K.D. Larsen, C. Lau, T.A. Lemon, A.J. Liang, Y. Liu, L.T. Luong, J. Michaels, J.J. Morgan, R.J. Morgan, M.T. Mortrud, N.F. Mosqueda, L.L. Ng, R. Ng, G.J. Orta, C.C. Overly, T.H. Pak, S.E. Parry, S.D. Pathak, O.C. Pearson, R.B. Puchalski, Z.L. Riley, H.R. Rockett, S.A. Rowland, J.J. Royall, M.J. Ruiz, N.R. Sarno, K. Schaffnit, N. V Shapovalova, T. Sivisay, C.R. Slaughterbeck, S.C. Smith, K.A. Smith, B.I. Smith, A.J. Sodt, N.N. Stewart, K.-R. Stumpf, S.M. Sunkin, M. Sutram, A. Tam, C.D. Teemer, C. Thaller, C.L. Thompson, L.R. Varnam, A. Visel, R.M. Whitlock, P.E. Wohnoutka, C.K. Wolkey, et al. 2007. Genome-wide atlas of gene expression in the adult mouse brain. *Nature*. 445:168–76.

Morrow, E.M., S.-Y. Yoo, S.W. Flavell, T.-K. Kim, Y. Lin, R.S. Hill, N.M. Mukaddes, S. Balkhy, G. Gascon, A. Hashmi, S. Al-Saad, J. Ware, R.M. Joseph, R. Greenblatt, D. Gleason, J.A. Ertelt, K.A. Apse, A. Bodell, J.N. Partlow, B. Barry, H. Yao, K. Markianos, R.J. Ferland, M.E. Greenberg, and C.A. Walsh. 2008. Identifying autism loci and genes by tracing recent shared ancestry. *Science (New York, N.Y.)*. 321:218–23.

Nakamura, N., S. Tanaka, Y. Teko, K. Mitsui, and H. Kanazawa. 2005. Four Na+/H+ exchanger isoforms are distributed to Golgi and post-Golgi compartments and are involved in organelle pH regulation. *The Journal of biological chemistry*. 280:1561–72.

Newpher, T.M., and M.D. Ehlers. 2008. Glutamate receptor dynamics in dendritic microdomains. *Neuron*. 58:472–97.

Numata, M., and J. Orlowski. 2001. Molecular cloning and characterization of a novel (Na+,K+)/H+ exchanger localized to the trans-Golgi network. *The Journal of biological chemistry*. 276:17387–94.

Ohgaki, R., N. Fukura, M. Matsushita, K. Mitsui, and H. Kanazawa. 2008. Cell surface levels of organellar Na+/H+ exchanger isoform 6 are regulated by interaction with RACK1. *The Journal of biological chemistry*. 283:4417–29.

Ohgaki, R., M. Matsushita, H. Kanazawa, S. Ogihara, D. Hoekstra, and S.C.D. van Ijzendoorn. 2010. The Na+/H+ exchanger NHE6 in the endosomal recycling system

is involved in the development of apical bile canalicular surface domains in HepG2 cells. *Molecular biology of the cell*. 21:1293–304.

Orlowski, J., and S. Grinstein. 2004. Diversity of the mammalian sodium/proton exchanger SLC9 gene family - Springer. *Pflügers Archiv European Journal of Physiology*. 447:549–565.

Park, M., J.M. Salgado, L. Ostroff, T.D. Helton, C.G. Robinson, K.M. Harris, and M.D. Ehlers. 2006. Plasticity-induced growth of dendritic spines by exocytic trafficking from recycling endosomes. *Neuron*. 52:817–30.

Reitz, C., J.H. Lee, R.S. Rogers, and R. Mayeux. 2011. Impact of genetic variation in SORCS1 on memory retention. *PloS one*. 6:e24588.

Rogaeva, E., Y. Meng, J.H. Lee, Y. Gu, T. Kawarai, F. Zou, T. Katayama, C.T. Baldwin, R. Cheng, H. Hasegawa, F. Chen, N. Shibata, K.L. Lunetta, R. Pardossi-Piquard, C. Bohm, Y. Wakutani, L.A. Cupples, K.T. Cuenco, R.C. Green, L. Pinessi, I. Rainero, S. Sorbi, A. Bruni, R. Duara, R.P. Friedland, R. Inzelberg, W. Hampe, H. Bujo, Y.-Q. Song, O.M. Andersen, T.E. Willnow, N. Graff-Radford, R.C. Petersen, D. Dickson, S.D. Der, P.E. Fraser, G. Schmitt-Ulms, S. Younkin, R. Mayeux, L.A. Farrer, and P. St George-Hyslop. 2007. The neuronal sortilin-related receptor SORL1 is genetically associated with Alzheimer disease. *Nature genetics*. 39:168–77.

Sin, W.-C., D.M. Moniz, M.A. Ozog, J.E. Tyler, M. Numata, and J. Church. 2009. Regulation of early neurite morphogenesis by the Na+/H+ exchanger NHE1. *The Journal of neuroscience : the official journal of the Society for Neuroscience*. 29:8946–59.

Stenmark, H. 2009. Rab GTPases as coordinators of vesicle traffic. *Nature reviews. Molecular cell biology*. 10:513–25.

Strømme, P., K. Dobrenis, R. V Sillitoe, M. Gulinello, N.F. Ali, C. Davidson, M.C. Micsenyi, G. Stephney, L. Ellevog, A. Klungland, and S.U. Walkley. 2011. X-linked Angelman-like syndrome caused by Slc9a6 knockout in mice exhibits evidence of endosomal-lysosomal dysfunction. *Brain : a journal of neurology*. 134:3369–83.

Tominaga, T., and D.L. Barber. 1998. Na-H exchange acts downstream of RhoA to regulate integrin-induced cell adhesion and spreading. *Molecular biology of the cell*. 9:2287–303.

Toro, R., M. Konyukh, R. Delorme, C. Leblond, P. Chaste, F. Fauchereau, M. Coleman, M. Leboyer, C. Gillberg, and T. Bourgeron. 2010. Key role for gene dosage and synaptic homeostasis in autism spectrum disorders. *Trends in genetics : TIG*. 26:363–72.

Xinhan, L., M. Matsushita, M. Numaza, A. Taguchi, K. Mitsui, and H. Kanazawa. 2011. Na+/H+ exchanger isoform 6 (NHE6/SLC9A6) is involved in clathrin-dependent endocytosis of transferrin. *American journal of physiology. Cell physiology*. 301:C1431–44. doi:10.1152/ajpcell.00154.2011.